11th International Symposium on Turbulence and Shear Flow Phenomena (TSFP11)
Southampton, UK, July 30 to August 2, 2019

USING A STOCHASTIC ONE-DIMENSIONAL TURBULENCE MODEL TO STUDY INCOMPRESSIBLE SPATIALLY DEVELOPING TURBULENT BOUNDARY LAYERS

Rakhi
Department of Mechanical Engineering
Electrical and Energy Systems
BTU Cottbus-Senftenberg
03046 Cottbus
rakhi.rakhi@b-tu.de

Heiko Schmidt
Department of Mechanical Engineering
Electrical and Energy Systems
BTU Cottbus-Senftenberg
03046 Cottbus
heiko.schmidt@b-tu.de

ABSTRACT

A map-based stochastic approach, One-Dimensional Turbulence (ODT), is applied to analyze the incompressible spatially developing turbulent boundary layer (SBL). The application of ODT to investigate the turbulent boundary layer is revisited for the spatial ODT formulation as it is physically more relevant. In the present preliminary study, the SBL canonical flow problem is formed by a plain moving wall and a free stream at rest. The flow variables are resolved on all scales along a 1-D domain. These variables are resolved by a deterministic process representing the molecular diffusion and a stochastic process modeling the effect of turbulent advection and pressure fluctuations. Due to the reduced dimensions in the model, it achieves major cost reductions as compared to the full 3-D simulations and is, thus, able to explore large parameter regimes. The simulations are presented for momentum thickness Reynolds number, $Re_\theta \approx 2000$ with $Re_\theta = U_b\theta/\nu$, where ν is the kinematic viscosity, U_b is the uniform velocity provided at the bottom wall and θ is the momentum layer thickness. We have analyzed various features related to the turbulent boundary layer, such as the mean, root mean square, skewness and flatness velocity profiles and the shape factor ae well as the skin friction coefficient using ODT and compared our results to the available reference Direct Numerical Simulations (DNS) and Large Eddy Simulations (LES) results. The comparison presented suggests that ODT is a reasonably accurate approach for the simulations of the spatially developing turbulent boundary layers.

INTRODUCTION

The study and understanding of turbulent boundary-layer-type flows are a major topic in research due to numerous applications in the atmospheric sciences, Engineering and industry. The spatial approach by Schlatter *et al.* (2009), Schlatter & Örlü (2010, 2012), and the temporal approach by Kozul *et al.* (2016) have been used to analyze the incompressible turbulent boundary layer. The spatially developing boundary layer (SBL) are inhomogeneous in the streamwise and wall-normal directions, which results in large computational requirements discussed by Schlatter *et al.* (2009), Schlatter & Örlü (2010), Spalart (1988), and Jiménez *et al.* (2010). Despite the computational limitations, the spatial approach is more relevant. The fully resolved 3-D simulations have been limited to small and moderate momentum Reynolds number discussed by Schlatter & Örlü (2012).

In the present paper, we utilize ODT by Kerstein (1999) and Kerstein *et al.* (2001) as stand-alone tool for the simulation of the SBL. Due to reduction of dimensionality, the model enables the simulation of high Reynolds number turbulence over the full range of dynamically relevant length scales. Although, it is difficult to capture all aspects of a full 3-D DNS with a reduced order model, it is interesting to check the predictability of the model for the simplest possible set-up. To investigate complex flows, ODT lines can be embedded in a coarse 3-D LES mesh referred to as ODTLES (Schmidt *et al.* (2003, 2010), Glawe *et al.* (2018)) removing the restriction to one dimension. In the present study we aim to validate the stand-alone model for the SBL by comparing the ODT results to the available reference DNS and LES data.

In the following, after providing a brief background of the model and simulation set-up used for the present case, we will compare ODT results to the DNS data by Schlatter & Örlü (2010) and LES data by Eitel-Amor *et al.* (2014). Firstly, we have discussed the variation of the structural properties i.e., the shape factor and the skin friction coefficient as a function of momentum thickness Reynolds numbers, Re_θ. Secondly, we have presented the velocity statistics up to fourth order for only one Re_θ (≈ 2000) case in comparison with the DNS data from Schlatter & Örlü (2010).

ODT MODEL FORMULATION

The original formulation of ODT was given by Kerstein (1999) and was later extended to include pressure scrambling effects (Kerstein *et al.* (2001)). The model was then gradually extended for the simulation of a variety of flows. Here we will highlight some important references which are, in general, important for the boundary layers. A limited validation of a case involving forcing of a boundary layer flow is presented by Lignell *et al.* (2013) and stably-stratified boundary layers by Kerstein & Wunsch (2006). Fragner & Schmidt (2017) presented an asymptotic suction boundary layer exhibiting a temporal evolution running into a statistical steady state. Further, the temporally developing turbulent boundary layer (TBL) has been investigated by Rakhi *et al.* (2018), which further motivated our present study for SBL due to its fundamental relevance.

Governing equations

In ODT, the governing equations are expressed in terms of two independent variables. There are two possible approaches regarding this matter, one approach considers the temporal ODT formulation (T-flow) and the another is the spatial ODT formulation (S-flow). In the present study, ODT models the spatial evolution of a 3-D turbulent flow field in a 1-D subspace, which is aligned with the wall-normal direction y. The density of the working fluid is constant. The spatial evolution of the velocity vector $u_i(y,x)$, where $u_i = u, v, w$ denotes the Cartesian components in the streamwise, wall-normal and spanwise directions (Lignell *et al.* (2013)), is described as

$$\frac{\partial[{u_i}^2(y,x)]}{\partial x} + EE[u_j(y,x)] = \nu \frac{\partial^2 u_i(y,x)}{\partial y^2}. \quad (1)$$

The first term of the above equation represents the local change of the velocity vector with respect to longitudinal direction x. The stochastic eddy event term EE, represents the effects of the turbulent advection and fluctuating pressure gradient forces due to turbulent eddy motions. The last term represents the viscous forces, which involves the kinematic viscosity ν and retain the Laplacian, though, restricted to the ODT-resolved dimension. For the spatial formulation, note that the mass flux is conserved instead of conserving the mass in cells.

Eddy events

Eddy events, the term EE in the above equation, occur through the instantaneous displacement of the fluid elements to represent a turbulent stirring motion. This modifies any property profile over the ODT line interval $y_0, y_0 + l$, where y_0 is the lower edge of a notional eddy and l its size. The implementation of the eddy events uses triplet map, which includes fluid displacement and fulfill two fundamental requirements: (i) the mapping is measure preserving, and (ii) it does not introduce spatial discontinuities. The triplet map essentially takes a scalar profile in an eddy region and replaces it with three copies of the original, each compressed by a factor of three, with the middle copy inverted in order to avoid the discontinuities (Kerstein (1999)). This corresponds to a physical mapping, that is, an advective, transport of fluid from a given location y to a new location $f(y)$ defined as (Kerstein (1999))

$$f(y) = y_0 + \begin{cases} 3(y-y_0), & y_0 \le y \le y_0 + l/3 \\ 2l - 3(y-y_0), & y_0 + l/3 \le y \le y_0 + 2l/3 \\ 3(y-y_0) - 2l, & y_0 + 2l/3 \le y \le y_0 + l \\ (y-y_0), & otherwise. \end{cases} \quad (2)$$

The mapped velocity field, $u_i(f(y),x)$, is further modified by the fluctuating pressure gradient forces with the aid of a kernel function defined as $K(y) = y - f(y)$, and three coefficients c_i, $u_i(y,x) \to u_i(f(y),x) + c_i K(y)$ (Kerstein *et al.* (2001)). $K(y)$ is by construction nonzero in the eddy-size interval $[y_0, y_0 + l]$ and it integrates to zero. The coefficients c_i are determined by considering the change of the kinetic energy ΔE_i in the ith velocity component (Kerstein *et al.* (2001)) given as

$$\Delta E_i = \frac{\rho}{2} \int_{y_0}^{y_0+l} \left(\left[u_i\big(f(y),x\big) + c_i K(y) \right]^2 - u_i^2(y,x) \right) \mathrm{d}y. \quad (3)$$

Energy conservation is achieved when the sum of the individual contributions vanishes, i.e., $\Delta E_1 + \Delta E_2 + \Delta E_3 = 0$. This constrains the selection of c_i since each velocity component has a finite amount of energy that can be removed and added to the other two components.

The extractable kinetic energies $(-\Delta E_i)$ are maximized with respect to the c_i in order to find an appropriate energy scale. This yields the maximum extractable energy, Q_i, given as

$$Q_i = \frac{1}{2\hat{K}} \rho l u_{i,K}^2, \quad (4)$$

where

$$u_{i,K} = \frac{1}{l^2} \int_{y_0}^{y_0+l} u_i\big(f(y),x\big) K(y) \, \mathrm{d}y, \quad (5)$$

and

$$\hat{K} = \frac{1}{l^3} \int_{y_0}^{y_0+l} K^2(y) \, \mathrm{d}y. \quad (6)$$

As mentioned by Kerstein *et al.* (2001), the pressure fluctuations may not be universal and that the pressure fluctuations do not necessarily imply a maximization of the inter-component kinetic energy transfer. Therefore, the model parameter α has been introduced to control the fraction of each of the extractable (available) kinetic energies that is actually used for the redistribution as

$$\Delta E_i = -\alpha Q_i + \frac{\alpha}{2} Q_j + \frac{\alpha}{2} Q_k, \quad (7)$$

where (ijk) are cyclic permutations of (123). The model parameter α takes values in the range $[0,1]$, where 0 means no and 1 maximal transfer of the kinetic energy and equipartition of the energies is approximated for $\alpha = 2/3$. Finally, the coefficients c_i are obtained by inserting Eqs. 4 and 7 in Eq. 3.

Eddy event selection

Eddy events have been formulated above, but it remains to determine their location y_0, size l, and streamwise position x of occurrence. These three stochastic variables are governed by an 'eddy rate distribution' $\lambda(y_0,l,x)$ Kerstein (1999), where $\lambda(y_0,l,x)\,\mathrm{d}y_0\,\mathrm{d}l\,\mathrm{d}x$ specifies the number of eddies in the size range $[l,l+\mathrm{d}l]$, position range $[y_0,y_0+\mathrm{d}y_0]$ and in a space interval $[x,x+\mathrm{d}x]$. The eddy position relates only to the region where turbulence is active such that λ can be rewritten on dimensional grounds as

$$\lambda(l,y_0,x) = \frac{C}{l^2\,\tau(l,y_0,x)}. \tag{8}$$

Here, τ is the eddy turnover time related to the instantaneous flow state and C is a proportionality constant related to the overall rate of eddy events in the flow. The latter is a model parameter that needs to be estimated for a given flow configuration since the turbulence intensity in general depends on the prescribed forcing mechanism.

To calculate τ, we consider the kinetic energy per unit mass l^2/τ^2 contained in the eddy motion. Consistency of the formulation demands that this energy is similar to the extractable kinetic energy as given in Eqs. 3 and 4 above. This yields

$$\frac{l^2}{\tau^2} \sim \sum_{i=1}^{3} u_{i,K}^2 - Z\frac{\nu^2}{l^2}. \tag{9}$$

Here, $u_{i,K}^2$ are summed instead of ΔE_i, showing that the total extractable kinetic energy does not depend on the inter-component energy transfer (model parameter α). The last term in Eq. 9 represents the damping effects of the viscosity. The corresponding model parameter Z takes values larger or equal to zero, where $Z=1$ effectively suppresses eddy events below the Kolmogorov scale (Kerstein (1999)). This parameter has been introduced originally to improve the numerical efficiency since such small eddy events do not contribute to the turbulent transport.

The eddy time scale τ is computed from the instantaneous velocity profiles $u_i(y,x)$, once the location y_0 and size l of an eddy event have been selected,

$$\frac{1}{\tau} = \sqrt{\frac{1}{l^2}\sum_{i=1}^{3} u_{K,i}^2 - Z\frac{\nu^2}{l^4}}. \tag{10}$$

The eddy time scale τ is in turn compared with the mean sampling time scale τ_s to obtain the acceptance probability $p_a = \tau/\tau_s \ll 1$ of a physically plausible eddy event. For this purpose, τ needs to be computed at a specific point in time that is obtained with the aid of a marked Poisson process. This process assumes that eddy events are independent of each other, such that the time increment between two such events can be sampled economically from an exponential distribution. We refer the reader to Kerstein (1999) for further details.

SIMULATION SET-UP

The spatial formulation of ODT allows simulations of flows that are statistically 2-D and the time dimension is replaced by evolution in a direction spatially orthogonal to the ODT line (Lignell *et al.* (2013)). The ODT computational domain is a line of size (height) D. The SBL is realized on this line by prescribing Dirichlet boundary condition at the bottom wall with $U_b = 12$ m/s and Neumann condition at the top wall. For practical reasons, we take the lower wall as moving and the free stream at rest. The velocity statistics are obtained on an ensemble basis using at least $N=1000$ members. These members are individual ODT realizations that can be run in parallel on a large computing cluster. All members are autonomous so that communication is not a limiting factor. An ensemble of different turbulent solutions is obtained from the same initial conditions by varying the seed of the underlying random number generator.

The streamwise velocity component u has been initialized using a laminar profile generated by solving diffusion part using the ODT model. The ODT laminar profile is similar to the laminar Blasius profile used to initiate the DNS results. The other velocity components (v,w) are initialized to zero. The simulations are carried out for different momentum Reynolds numbers, $Re_\theta = \theta U_b/\nu$, where θ is the momentum layer thickness and the kinematic viscosity ν of the working fluid is fixed as $\nu = 1.5\times10^{-5}\,\mathrm{m^2/s}$ (air). In the present paper we have presented the analyses only for $Re_\theta \approx 2000$. The domain size D has been selected such that it is constant in bulk units ν/U_b, that is, $DU_b/\nu = 45{,}000$ (or 100 in terms of $\delta^\star$, which is the displacement thickness).

Eddy events are efficiently sampled from empirical distributions. The specific choice does not change the results as long as the physically relevant range-of-scales is permitted as discussed by Kerstein (1999). In the present implementation (Lignell *et al.* (2013)), three numerical parameters are needed: the maximum (L_{max}), minimum (L_{min}), and most probable (L_p) eddy size. The maximum eddy size has been selected as $L_{max}U_b/\nu = 27{,}000$, which corresponds to 60% of the domain size. This aids the numerical efficiency. The minimum eddy size, L_{min}, is estimated from the Kolmogorov length scale with the aid of pre-simulations. For the most probable eddy size we have used $L_p = 3L_{min}$ to capture the initial transient stage.

At last, we note that a dynamic adaptive mesh by Lignell *et al.* (2013) is used to carry out the simulations. This demands the specification of several more numerical parameters but here we have used the default values for most of them. The most important adaptivity parameters control the size range of the cells and the frequency of mesh adaptations. The minimum and maximum allowed grid cell sizes must be spaced sufficiently from each other for the dynamic mesh adaption procedure (Lignell *et al.* (2013)). Here we have used the minimum and maximum grid cell sizes of the reference DNS by Schlatter & Örlü (2010). The physical model parameters, $\alpha = 2/3$, $C=6$ and $Z=600$ are used for the simulations of the SBL configurations. The selection procedure for these parameters is not in the scope of the present paper. Note that we follow the usual convention and denote the variables rescaled to the viscous units with the superscript '+', for example, $u^+ = u/u_\tau$ and $y^+ = y/y_\tau$, where u_τ is the frictional velocity ($u_\tau = \sqrt{\tau_0/\rho}$ with $\tau_0 \equiv -\mu\partial\overline{u}/\partial y\,|_0 > 0$) and y_τ is the viscous reference length scale ($y_\tau = \nu/u_\tau$).

Variation of the structural properties with momentum Reynolds numbers

For SBL, the ODT structural properties, i.e., the shape factor (H) and the skin friction coefficient (C_f) with Re_θ

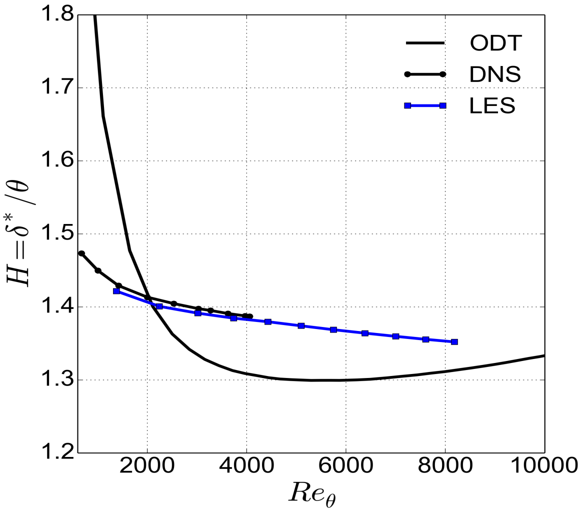

Figure 1. The quantity H as a function of Re_θ up to $Re_\theta \approx 10000$. For comparison, the reference DNS data from Schlatter & Örlü (2010) and LES data from Eitel-Amor *et al.* (2014) is shown.

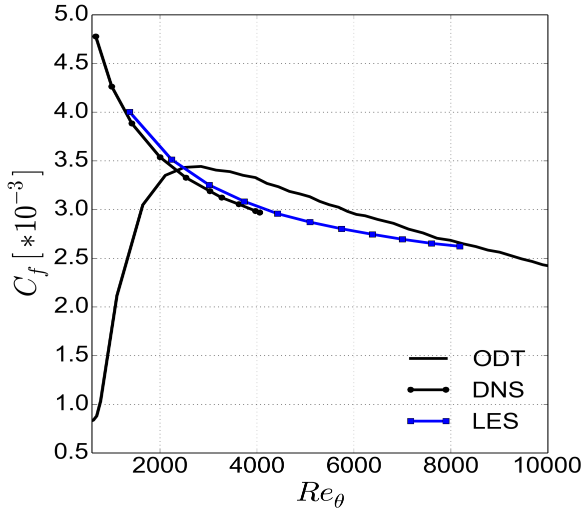

Figure 2. Skin friction coefficient C_f as a function of Re_θ. For comparison, the reference DNS data from Schlatter & Örlü (2010) and LES data from Eitel-Amor *et al.* (2014) is shown.

are discussed in this section. For comparison, the reference DNS data from Schlatter & Örlü (2010) up to $Re_\theta \approx 4300$ and LES data from Eitel-Amor *et al.* (2014) up to $Re_\theta \approx 8300$ is also plotted for the structural properties.

The shape factor (H) is the ratio of the displacement thickness and momentum thickness, i.e., $H = \delta/\theta$, and is plotted with Re_θ in Figure 1. It gives a direct quantitative estimation of the mean streamwise velocity profile independent of the skin friction. The figure also displays the DNS up to $Re_\theta \approx 4300$ and the LES data up to $Re_\theta \approx 8300$ from Schlatter & Örlü (2010); Eitel-Amor *et al.* (2014). Although, we see a convergence of the shape factor at higher Re_θ but the ODT data does not show good agreement with the reference data. In the small Re_θ range we report a different Re_θ trend and in the range from $2000 < Re_\theta < 8000$, ODT under-predicts the value for the shape factor in comparison with the DNS as well as LES data. Nevertheless, it is worth noting the behaviour for this property for a reduced order model.

Figure 2 shows the development of the skin friction coefficient, $C_f = 2/(U_b^+)^2$, with Re_θ. C_f is defined as the ratio of the wall shear stress to the dynamic pressure. The behaviour in case of SBL is very much similar to TBL reported in Rakhi *et al.* (2018). Initially, the profile for ODT shows deviation from the DNS and LES data, although as it reaches the final turbulent equilibrium state, it finally tends towards the reference data, showing asymptotic insensitivity to the initial conditions. The behavior of C_f is similar to the DNS and LES profiles reported by Schlatter & Örlü (2010); Eitel-Amor *et al.* (2014) form $Re_\theta \approx 2500$ onward with a slight under-prediction of the C_f using ODT methodology. However, in the small Re_θ range we observe an inconsistent trend with respect to Re_θ in case of the reduced order model in comparison with the reference data. The C_f peak amplitude could be modified by changing the model parameters. With the chosen combination of parameters, however, the qualitative trends are sufficiently well reproduced, as well as the collapse into the fully turbulent state along with the lower and higher order statistics, thus confirming the predictive capabilities of ODT.

VELOCITY STATISTICS

The predictive capabilities of ODT are addressed in this section by keeping the fixed bulk velocity. The physical model parameters are frozen for this purpose at $\alpha = 2/3$, $C = 6$ and $Z = 600$. The ODT simulation results up to the fourth order velocity statistics are discussed and compared to the available reference DNS results of Schlatter & Örlü (2010) at $Re_\theta \approx 2000$.

Velocity statistics up to second order

Figure 3 (left) displays the mean streamwise velocity profile as a function of the wall-normal coordinate in viscous units at $Re_\theta \sim 2000$ along with the DNS reference from Schlatter & Örlü (2010). We have $U_b^+ - \overline{u}^+$ on y-axis due to the simulation set up used in the present study. The ODT profile shows very good agreement with the DNS data with very slight deviation only in the outer-log region. This shows the ability of ODT to capture transitions from the inner to the buffer layer, and further into the log-region.

The root mean square (rms) of the normalized streamwise velocity component ($u^+_{rms} = \sqrt{\overline{u'^2}}/u_\tau$) as a function of normalized wall-normal coordinate in viscous units is depicted in Figure 3 (right) at $Re_\theta \sim 2000$. The peak amplitude is under-predicted by ODT compared to the DNS data. This peak can be optimized by choosing small value of the model parameter C, but in that case the velocity profile tends towards a laminar profile. This ODT feature has already been reported in the literature by Schmidt *et al.* (2003), and can be avoided by retaining some 3-D information of the flow.

The double peak arising near to the wall, $y^+ \approx 10$, represents an artifact generated by the topology of the triplet map close to the wall. This is explained in more detail by Lignell *et al.* (2013). Although the peak is under-predicted for rms, some general trends from the DNS data from Schlatter & Örlü (2010) are confirmed with the ODT for the given initial condition and for the chosen physical parameters.

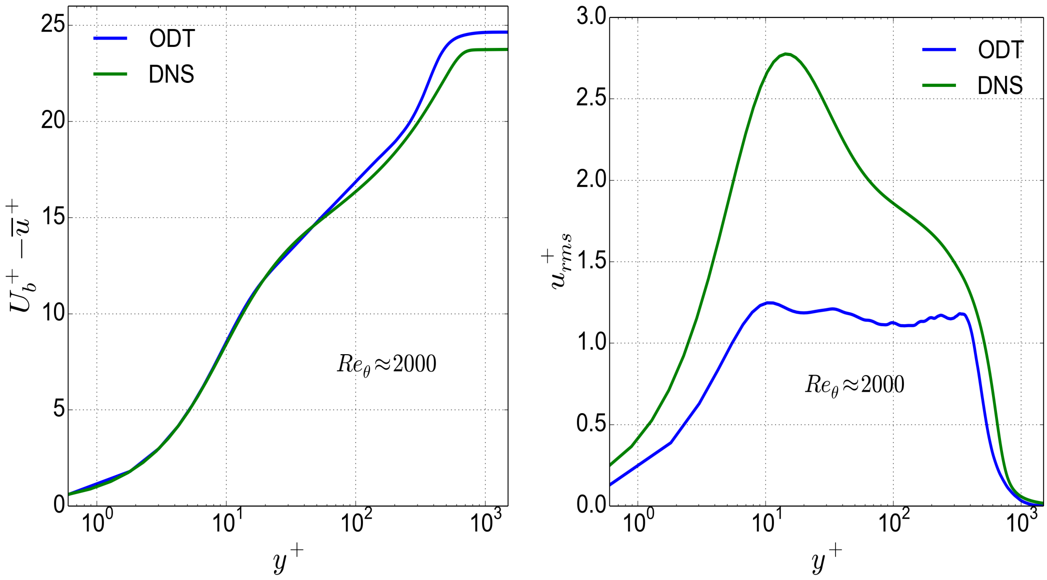

Figure 3. Left: The mean streamwise velocity profile; Right: The root mean square velocity profile, as a function of wall-normal coordinate (in viscous units) at $Re_\theta \approx 2000$. For reference, DNS data is plotted from Schlatter & Örlü (2010).

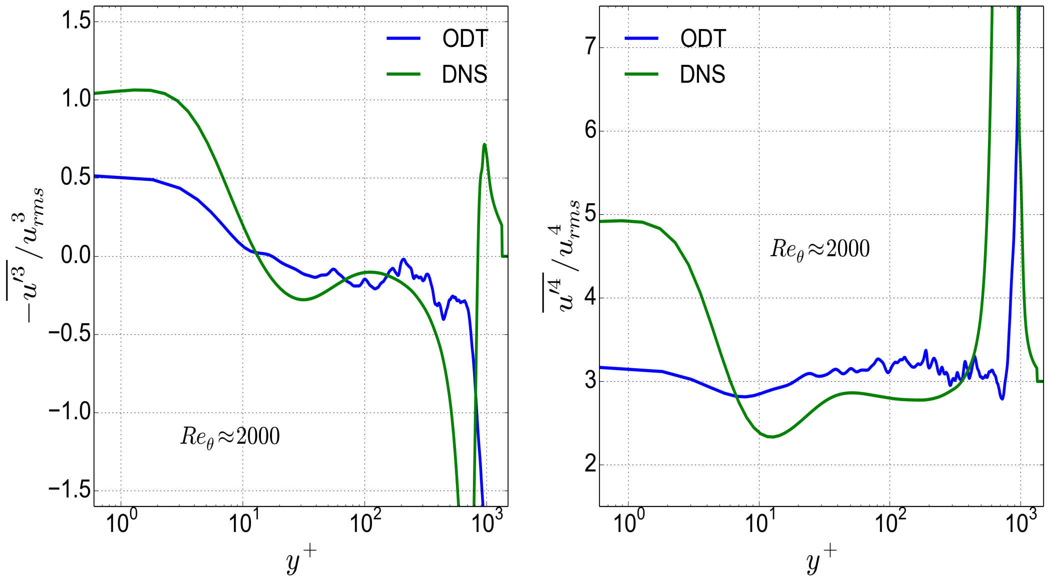

Figure 4. Left: Skewness and Right: Flatness, of the streamwise velocity component as a function of wall normal coordinate (in viscous units) at $Re_\theta \approx 2000$. For reference, DNS data from Schlatter & Örlü (2010) is shown.

Velocity statistics up to fourth order

The skewness of the streamwise velocity component, $-\overline{u'^3}/u^3_{rms}$, as a function of wall-normal coordinate (in viscous units) at $Re_\theta \sim 2000$ is depicted in Figure 4 (left). It can be seen that the ODT model tends to over-predict the positive skewness near the wall i.e. $y^+ < 10$. The skweness profile show agreement with the reference DNS in the outer region between $10 < y^+ < 500$. However, there are large disagreements and very different trends in the outer-log region, where DNS profiles exhibit a sudden increase in the skewness values. This feature is not captured by ODT, and is presumably attributed to the missing 3-D coherent structure information. This figure also illustrates the potential of ODT to calculate the third order velocity statistics. A similar behaviour was observed for a TBL using ODT (Rakhi *et al.* (2018)). The ODT profiles are qualitatively consistent with the DNS data.

Figure 4 (right) shows the flatness of the streamwise velocity component, $\overline{u'^4}/u^4_{rms}$, as a function of wall-normal coordinate at $Re_\theta \sim 2000$. ODT highly under-predicts the fourth-order velocity statistics in the inner region near the wall, i.e., $y^+ < 8$. The flatness in case of SBL, is over-predicted in the region between $8 < y^+ < 600$. However, in case of TBL, this region was reported as $10 < y^+ < 80$. A Gaussian flatness with a value close to three is observed close to the wall for the ODT results. In general, ODT is more Gaussian than the DNS, which we attribute to the 3-D eddy motions and vortex stretching which leads to inhomogeneity but remains unresolved in ODT. The full 3-D instabilities and coherent structures exhibited by the DNS, are completely absent in the stochastic picture of ODT. The profile do not show good agreement with the DNS data. As explained for rms profiles, in case of flatness as well, we might need to retain some 3-D information in a non-standalone application of ODT in order to reproduce fourth-order velocity statistics to overcome this limitation (Schmidt *et al.*, 2003, 2010), (Glawe *et al.*, 2018) and, thus, allowing simulations of much more complex flows.

CONCLUSIONS

In the present paper, we apply the ODT model for the first time to investigate the incompressible spatially developing turbulent boundary layer. The model resolves the flow variables along a 1-D computational domain in which the viscosity effects are represented by the deterministic diffusion equation and the turbulent advection by stochastic mapping events. We compare the velocity statistics such as mean, root mean square, skewness and flatness as wall-normal profiles produced from ODT to the reference DNS data from Schlatter & Örlü (2010) at $Re_\theta \approx 2000$. The key findings of the preliminary study are summarized as follows:

1. The mean streamwise velocity matches to the reference DNS results up to a good degree showing that the model is able to capture flow dynamics ranging from the viscous sublayer through the buffer layer and into the logarithmic layer.
2. The peak amplitude of the root mean square velocity profiles is under-predicted compared to the reference data confirming the known limitation of the model reported earlier by Kerstein (1999); Kerstein *et al.* (2001); Lignell *et al.* (2013), which may be alleviated by retaining 3-D information.
3. The skewness of the streamwise velocity component is slightly under-predicted in the inner region, over-predicted in the buffer region and we see disagreement in the outer region for the SBL solution.
4. The flatness of the streamwise velocity component is only reproduced in a certain region by using the reduced-order formulation. As commented before, capturing higher order statistics may require retaining some 3-D information.

The major focus of the model is representing the dynamics close to the wall in the boundary layers and ensure the qualitative reproducibility of the velocity statistics up to third order. The ODT model achieves considerable cost reduction as compared to the full 3-D simulations. The comparison presented here suggested that ODT is able to reproduce several DNS velocity statistics for the incompressible spatially developing turbulent boundary layers which makes ODT an interesting tool for the investigation of boundary-layer-type flows for high Reynolds numbers.

REFERENCES

Eitel-Amor, G., Örlü, R. & Schlatter, P. 2014 Simulation and validation of a spatially evolving turbulent boundary layer up to $R_\theta = 8300$. *International Journal of Heat and Fluid Flow* **47**, 57–69.

Fragner, M. M. & Schmidt, H. 2017 Investigating asymptotic suction boundary layers using a one-dimensional stochastic turbulence model. *Journal of Turbulence* **18**, 899–928.

Glawe, C., Medina M., J. A. & Schmidt, H. 2018 IMEX based multi-scale time advancement in ODTLES. *Zeitschrift für Angewandte Mathematik und Mechanik* **98**, 1907–1923.

Jiménez, J., Hoyas, S., Simens, M. P. & Mizuno, Y. 2010 Turbulent boundary layers and channels at moderate Reynolds numbers. *Journal of Fluid Mechanics* **657**, 335–360.

Kerstein, A. 1999 One-dimensional turbulence: model formation and application to homogeneous turbulence, shear flows, and buoyant stratified flows. *Journal of Fluid Mechanics* **392**, 277–334.

Kerstein, A., Ashurst, W., Wunsch, S. & Nilsen, V. 2001 One-dimensional turbulence: vector formulation and application to free shear flows. *Journal of Fluid Mechanics* **447**, 85–109.

Kerstein, A. R. & Wunsch, S. 2006 Simulation of a stably stratified atmospheric boundary layer using one-dimensional turbulence. *Boundary Layer-Meteorology* **118**, 325–356.

Kozul, M., Chung, D. & Monty, J. P. 2016 Direct numerical simulation of the incompressible temporally developing turbulent boundary layer. *Journal of Fluid Mechanics* **796**, 437–472.

Lignell, D., Kerstein, A., Sun, G. & Monson, E. 2013 Mesh adaption for efficient multiscale implementation of One-Dimensional Turbulence. *Theoretical and Computational Fluid Dynamics* **27**, 273–295.

Rakhi, Klein, M., Medina M., J. A. & Schmidt, H. 2018 One-dimensional turbulence modeling of incompressible temporally developing turbulent boundary layers with comparison to DNS. *Journal of Turbulence* (Submitted).

Schlatter, P. & Örlü, R. 2010 Assessment of direct numerical simulation data of turbulent boundary layers. *Journal of Fluid Mechanics* **659**, 116–126.

Schlatter, P. & Örlü, R. 2012 Turbulent boundary layers at moderate Reynolds number: inflow length and tripping effects. *Journal of Fluid Mechanics* **710**, 5–34.

Schlatter, P., Örlü, R., Li, Q., Brethouwer, G., Fransson, J. H. M., Johansson, A. V., Alfredsson, P. H. & Henningson, D. S. 2009 Turbulent boundary layers up to $R_\theta = 2500$ studied through simulation and experiment. *Physics of Fluid* **21**, 051702–1–051702–4.

Schmidt, R., Kerstein, A. & McDermott, R. 2010 ODTLES: A multi-scale model for 3D turbulent flow based on one-dimensional turbulence modeling. *Computer Methods in Applied Mechanics and Engineering* **199**, 865–880.

Schmidt, R., Kerstein, A. R., Wunsch, S. & Nilsen, V. 2003 Near-wall LES closure based on one-dimensional turbulence modeling. *Journal of Computational Physics* **186**, 317–355.

Spalart, P. R. 1988 Direct simulation of a turbulent boundary layer up to $R_\theta = 1410$. *Journal of Fluid Mechanics* **187**, 61–98.